Open Access Full Text Article

ORIGINAL RESEARCH

Luteolin decreases invasiveness, deactivates STAT3 signaling, and reverses interleukin-6 induced epithelial–mesenchymal transition and matrix metalloproteinase secretion of pancreatic cancer cells

Xince Huang[1]
Shengjie Dai[1]
Juji Dai[1]
Yuwu Xiao[1]
Yongyu Bai[1]
Bicheng Chen[1,2]
Mengtao Zhou[1]

[1]Department of Surgery, The First Affiliated Hospital, Wenzhou Medical University, Wenzhou, Zhejiang Province, People's Republic of China; [2]Zhejiang Provincial Top Key Discipline in Surgery, Wenzhou Key Laboratory of Surgery, Wenzhou, Zhejiang Province, People's Republic of China

Correspondence: Mengtao Zhou;
Bicheng Chen
Department of Surgery, The First Affiliated Hospital, Wenzhou Medical University, 2 Fuxue Lane, Wenzhou 325000, Zhejiang Province, People's Republic of China
Email zmt0417@hotmail.com

Abstract: Luteolin, a flavone, has been shown to exhibit anticancer properties. Here, we investigated whether luteolin affects epithelial–mesenchymal transition (EMT) and invasiveness of pancreatic cancer cell lines and their underlying mechanism. Pancreatic cancer cell lines PANC-1 and SW1990 were used in our study, and their EMT characters, matrix metalloproteinase (MMP) expression level, invasiveness, and signal transducer and activator of transcription 3 (STAT3) activity were determined after luteolin treatment. We also treated pancreatic cancer cells with interleukin-6 (IL-6) to see whether IL-6-induced activation of STAT3, EMT, and MMP secretion was affected by luteolin. We found that luteolin inhibits EMT and MMP2, MMP7, and MMP9 expression in a dose-dependent manner, similar to STAT3 signaling. Through Transwell assay, we found that invasiveness of pancreatic cancer cells was inhibited by luteolin. EMT characters and MMP secretion increase with STAT3 activity after IL-6 treatment and these effects, caused by IL-6, were inhibited by luteolin. We concluded that luteolin inhibits invasiveness of pancreatic cancer cells, and we speculated that luteolin inhibits EMT and MMP secretion likely through deactivation of STAT3 signaling. Luteolin has potential antitumor effects and merits further investigation.

Keywords: epithelial–mesenchymal transition, matrix metalloproteinase, luteolin, STAT3

Introduction

Flavonoids are polyphenolic compounds that are extensively found in food plants.[1,2] They have been proven to be the effective constituents of many plants and herbs used in traditional Chinese medicine and have preventive and therapeutic effects against some diseases.[3] Luteolin, a flavone widely found in many food plants and herbs, has been identified as one of the most potent flavonoids in vitro and in vivo.[4,5] With many biological activities and therapeutic effects, including anti-inflammatory, proapoptosis, and reverse antineoplastic drug resistance, luteolin demonstrates a potential for treatment of inflammatory and neoplastic diseases.[6–10] A variety of effects, such as proapoptosis and cell cycle arrest, matrix metalloproteinase (MMP) suppression, and angiogenesis inhibition, have been uncovered as means of luteolin anticancer activities in vivo and in vitro.[9,11–13] In our study, we aimed at revealing luteolin's effect on inhibiting epithelial–mesenchymal transition (EMT) and on the invasiveness of pancreatic cancer, and their relationships with dephosphorylation of signal transducer and

activator of transcription 3 (STAT3), which is an important activity of luteolin in signal transduction.

EMT can be isolated during embryonic development, chronic inflammation, and cancer metastasis; it is a biologic process in which epithelial cells transform into special cells with mesenchymal phenotypes. The hallmark of EMT is changes in the expression of adhesion molecules, ie, upregulation of N-cadherin and the downregulation of E-cadherin.[14,15] Many other biomarkers also change during the EMT process, for example, upregulation of ZEB1 and upregulation of vimentin.[16,17] EMT markers are predictive for increased invasion, loss of differentiated characteristics, metastasis, and poor prognosis in a number of human tumor types.[18]

MMP is an enzyme family whose substrates are various kinds of extracellular matrix protein components. MMPs promote cancer cell migration by degrading the extracellular matrix, and they show a close relationship with tumor invasiveness and metastasis in pancreatic cancer.[19,20] Among more than 20 types of MMPs, MMP-2, MMP7, and MMP-9 have been proven to be involved in the aggressiveness of pancreatic cancer.[20–22]

Although its mechanism has not been fully clarified, stimulation with interleukin-6 (IL-6) has been confirmed as a process to induce EMT.[23,24] Some evidence shows that STAT3 is involved in the induction of EMT by IL-6.[25] In our research, we used IL-6 to activate STAT3, increase MMP secretion, and induce changes in EMT biomarkers to see whether luteolin reverses IL-6-induced EMT and inhibits IL-6-induced MMP secretion.

STAT3, a protein that is encoded by a gene located on chromosome 17, is phosphorylated by receptor-associated kinase and then forms homo- or heterodimers that translocate to the nucleus, where they function as transcriptional factors. STAT3 is activated by a variety of cytokines, growth factors, and hormones, such as leukemia inhibitory factor, IL-10, and so far the most important of all, IL-6.[26,27] After being activated, STAT3 mediates the expression of a variety of genes, among which many are associated with cellular proliferation, apoptosis, and malignant transformation.[28,29] Furthermore, it has been confirmed that STAT3 plays a critical role in K-ras-dependent pancreatic carcinogenesis.[20,30,31] Therefore, STAT3 and its associated pathways are thought to be increasingly important in cancer research and as potential factors in clinical cancer treatment.

In our study, we investigated luteolin's effects on invasiveness of pancreatic cancer cells. We also sought to confirm that luteolin reverses IL-6-induced EMT and MMP secretion.

And, we speculated that luteolin inhibits EMT and MMP secretion likely through deactivation of STAT3 signaling.

Materials and methods

The ethics were reviewed and approved by the board of Wenzhou Medical University. PANC-1 and SW1990 human pancreatic cancer cell lines were purchased from the Institute of Biochemistry and Cell Biology, the Chinese Academy of Science (Shanghai, People's Republic of China). Fetal bovine serum (FBS) was purchased from Sigma Chemical (St Louis, MO, USA). Roswell Park Memorial Institute (RPMI)-1640, Dulbecco's Modified Eagle's Medium (DMEM), and trypsin were purchased from GIBCO (Grand Island, NY, USA). Polymerase chain reaction (PCR) primers were purchased from Generay Biotech (Shanghai, People's Republic of China). Anti-phospho-STAT3 (Tyr705), anti-STAT3, anti-E-Cadherin, anti-N-Cadherin, anti-Vimentin, anti-Snail, anti-ZEB1/TCF8, anti-MMP2, and anti-MMP9 antibodies were purchased from Cell Signaling Technology (Danvers, MA, USA). Anti-GAPDH-antibody was purchased from Bioworld Technology (St Louis Park, MN, USA). Anti-MMP7 antibody was purchased from Santa Cruz Biotechnology, Inc. (Santa Cruz, CA, USA). Luteolin was purchased from MUST Bio-Technology (Chengdu, People's Republic of China). Power SYBR Green PCR Master Mix was purchased from Applied Biosystems (Foster City, CA, USA) and a RevertAid First Strand cDNA Synthesis Kit was purchased from Toyobo Co., Ltd. (Osaka, Japan).

Luteolin was dissolved in dimethylsulfoxide (DMSO) at a concentration of 100 mM and then added to the medium at the indicated concentrations to limit the DMSO concentration below 0.1%. Primary antibodies were diluted in primary antibody dilution buffer (Solarbio, Beijing, People's Republic of China) according to the instructions. Primers were dissolved in diethylpyrocarbonate water at the indicated concentration.

Cell culture

Human pancreatic cancer cell line PANC-1 was cultured in DMEM, and human pancreatic cancer cell line SW1990 was cultured in RPMI-1640 medium. Both media contained 10% FBS, 100 U/mL penicillin, and 100 µg/mL streptomycin. Cells were cultured at 37°C with 5% CO_2. Medium was changed every 2 days and cells were detached with 0.25% trypsin-0.02% ethylenediaminetetraacetic acid.

Cell treatment

PANC-1 and SW1990 cell lines were plated into 6-cm culture dishes. When cells reached 70%–90% confluence,

they were lysed for protein and RNA extraction or detached for Transwell invasion assay. IL-6 was added to FBS-free medium at a concentration of 100 ng/mL 72 hours before lysis or detachment; FBS-free medium was changed every 24 hours. Luteolin was added 24 hours before lysis or detachment at indicated concentrations.

Cell viability detection by Cell Counting Kit 8 assay

PANC-1 and SW1990 cells were plated into 96-well plates with each well containing approximately 5,000 cells. After 24 hours incubation, medium was changed and FBS-free medium with different concentration of luteolin was added into each well. Twenty-four hours later, medium containing luteolin was discarded and 100 μL FBS-free medium containing 10 μL Cell Counting Kit 8 (CCK8; Dojindo, Kumamoto, Japan) was added into each well. Then the cells were incubated for another 2 hours and absorbance at 490 nm of each well was detected by an enzyme-linked immunosorbent assay reader (BioTek, Winooski, VT, USA) according to the manufacturer's instructions. Cell viability was expressed as fold change of absorbance at 490 nm.

Transwell invasion assay and cell counting

Invasiveness of PANC-1 and SW1990 cells was investigated using 24-well BioCoat cell culture inserts (BD Biosciences, Franklin Lake, NJ, USA) with an 8 μm porosity polyethylene terephthalate membrane coated with Matrigel Basement Membrane Matrix (Corning, Franklin Lake, NJ, USA). The lower compartment contained RPMI-1640 (for SW1990) or DMEM (for PANC-1) with 10% FBS as a chemoattractant. After cell treatment, 10^5 cells in 0.2 mL FBS-free medium with 0.2% bovine serum albumin were placed in the upper compartment and incubated for 24 hours. After incubation, cells on the upper surface of the filter were gently scraped off; the filters were washed with phosphate-buffered saline (PBS) thrice and then fixed with 4% paraformaldehyde for 20 minutes. Subsequently, cells were stained with crystal violet. Cells that penetrated through the Matrigel to the lower surface of the filter were counted under a microscope.

Western blotting analysis

After treatment, cells were lysed by radioimmunoprecipitation assay lysis buffer with 10% phosphatase inhibitor and 1% phenylmethylsulfonyl fluoride for 30 minutes. Then, total protein lysate was centrifuged and the supernatant was collected. The protein concentration of each group of supernatant was measured. Fifty micrograms of total

protein for each group was resolved by sodium dodecyl sulfate–polyacrylamide gel electrophoresis using a 10% polyacrylamide gel. The separated protein on the gel was electrophoretically transferred to a polyvinyl difluoride membrane, which then was blocked with 5% skim milk in tris-buffered saline (10 mmol/L Tris-HCl, pH 8.0, containing 150 mmol/L NaCl and 0.1% Tween-20) for 1.5 hours at room temperature, followed by incubation with the primary antibodies against STAT3 (1:2,000), phospho-STAT3 (Tyr705; 1:1,000), E-cadherin (1:1,000), N-cadherin (1:1,000), vimentin (1:1,000), Snail (1:1,000), ZEB1 (1:1,000), MMP2 (1:1,000), MMP7 (1:200), MMP9 (1:1,000), and GAPDH (1:5,000) at 4°C overnight. After washing, the membranes were incubated with the appropriate horseradish peroxidase-conjugated secondary antibody to detect bands using Amersham™ ECL™ Prime (GE Healthcare, Little Chalfont, UK). The densities of the specific protein bands were visualized and captured by ImageQuant™ 400 (GE Healthcare).

RNA extraction and real-time PCR

Total RNA was extracted using Trizol (Invitrogen, Carlsbad, CA, USA) according to the manufacturer's protocol. cDNA was synthesized using 1 μg of total RNA in a 20 μL final volume by reverse transcription with oligo-dT(18)-primers. Real-time PCR (RT-PCR) reactions were performed using SYBR-Green Master Mix kit according to the manufacturer's instructions (Applied Biosystems). The RNA of STAT3, CDH1 (E-cadherin), CDH2 (N-cadherin), vimentin, ZEB1, Snail, MMP2, MMP7, and MMP9 was amplified using ABI Prism 7500 Sequence Detection System (Applied Biosystems). GAPDH was amplified as an internal standard. Primer sequences are listed in Table 1.

Immunofluorescence microscopy

Pancreatic cancer cell lines PANC-1 and SW1990 were plated onto six-well plates containing glass coverslips and allowed to adhere for 24 hours. Following cell treatment, cells were washed thrice with PBS and then fixed in 4% formaldehyde for 20 minutes. Fixed cells were then permeabilized in 0.2% Triton X-100, washed with PBS, and blocked with 5% goat serum for 1 hour at room temperature. Then, the samples were incubated with anti-E-cadherin antibody for 24 hours at 4°C, followed by incubation with a secondary antibody conjugated with Alexa Fluor 488 (ThermoFisher Scientific, Waltham, MA, USA) and DAPI to detect E-cadherin and cell nuclei. The coverslips were mounted with mounting media on microscope slides and the images visualized by

Table 1 The primers used for real-time PCR

Gene	Sense (5′–3′)	Antisense (5′–3′)
CDH1	TCACGCTGTGTCATCCAACGG	TAGGTGTTCACATCATCGTCCGC
CDH2	CATCATCATCCTGCTTATCCTTGT	GGTCTTCTTCTCCTCCACCTTCTT
Vimentin	AATCCAAGTTTGCTGACCTCTCTGA	ACTGCACCTGTCTCCGGTACTC
Snail	CTTCTCCTCTACTTCAGTCTCTTCC	TGAGGTATTCCTTGTTGCAGTATTT
ZEB-1	CGCTTCTCACACTCTGGGTCTTATT	CCTCTTCCCTTGTAAACTCTCT
MMP2	GGGGGAAGATGCTGCTGTT	AGCGGTCCTGGCAGAAATAG
MMP7	AGTGAGCTACAGTGGGAACAGGC	CATTATTTCTATGACGCGGGAGT
MMP9	CAGTCCACCCTTGTGCTCTTCC	CATCTCTGCCACCCGAGTGTAAC
STAT3	ACCAACAATCCCAAGAATGTAAACT	CATGTGATCTGACACCCTGAATAAT
GAPDH	GGGTGTGAACCATGAGAAGTATG	GATGGCATGGACTGTGGTCAT

Abbreviation: PCR, polymerase chain reaction.

fluorescence microscopy (Leica, DM4000B, Leica Micro-systems, Wetzlar, Germany).

Statistical analysis

Data are expressed as mean values ± standard deviation. Comparisons among multiple groups were made with a one-way analysis of variance followed by least significant difference or Dunnett's t-test. A value of $P < 0.05$ was considered to be statistically significant.

Results

Luteolin decreases cell viability and inhibits EMT in PANC-1 and SW1990 cell lines in a dose-dependent manner

At the beginning of our study, we performed CCK8 assay to see whether luteolin affects cell viability of PANC-1 and SW1990 cells. Both cell lines were treated with luteolin at concentration of 0, 20, 40, 80, 160, and 320 μM for 24 hours. Then, CCK8 assay was performed to detect cell viability. We found that cell viability did not decrease significantly at concentrations of 20 and 40 μM. When the concentration reached 80 and 160 μM, cell viability decreased significantly. But compared with the 0 μM group, both cell lines had more than 75% relative cell viability at the concentration of 160 μM. When luteolin concentration reached 320 μM, cell viability of both cell lines decreased drastically (Figure 1A).

According to the results of cell viability assay, 0, 20, 40, 80, and 160 μM of luteolin concentrations were chosen for further study. To avoid massive cell death, the concentration of 320 μM was not used. To investigate whether luteolin affects EMT characters of normal PANC-1 and SW1990 cells, we treated both cell lines with luteolin under concentrations of 0, 20, 40, 80, and 160 μM for 24 hours. An immunofluorescence assay was then performed to determine the cellular protein level of E-cadherin. With increasing luteolin concentration, E-cadherin expression increased accordingly (Figure 1B).

To more rigorously verify the effect of luteolin, RT-PCR was performed to determine the cellular messenger RNA (mRNA) levels of CDH1 (E-cadherin), CDH2 (N-cadherin), vimentin, ZEB1, and Snail. After 24 hours of luteolin treatment, both PANC-1 and SW1990 cells showed increased mRNA expression of CDH1 and decreased expression of CDH2, vimentin, ZEB1, and Snail in a dose-dependent manner (Figure 1C and D).

We also performed Western blotting assays to determine the protein level of EMT markers. In agreement with the results of RT-PCR, Western blotting assay showed that luteolin increased the protein level of E-cadherin and decreased N-cadherin, vimentin, Snail, and ZEB1 in a dose-dependent manner (Figure 1E).

Luteolin inhibits MMP secretion and pancreatic cancer cell invasiveness in a dose-dependent manner

Since MMPs have a close relationship with EMT, we next investigated whether luteolin could also inhibit MMP expression as mesenchymal markers. We treated PANC-1 and SW1990 cells with luteolin at concentrations of 0, 20, 40, 80, and 160 μM for 24 hours. After cell treatment, Western blotting and PCR assays were performed to determine protein and RNA levels of MMP2, MMP7, and MMP9. As expected, with increasing luteolin concentration, protein and RNA levels of MMP2, MMP7, and MMP9 decreased accordingly (Figure 2A–C).

As MMPs promote cancer cell invasion by degrading the extracellular matrix, we then measured the invasiveness of cancer cells after luteolin treatment with 24-well BioCoat cell culture inserts with an 8 μm porosity polyethylene terephthalate membrane. After Transwell assay, we randomly took
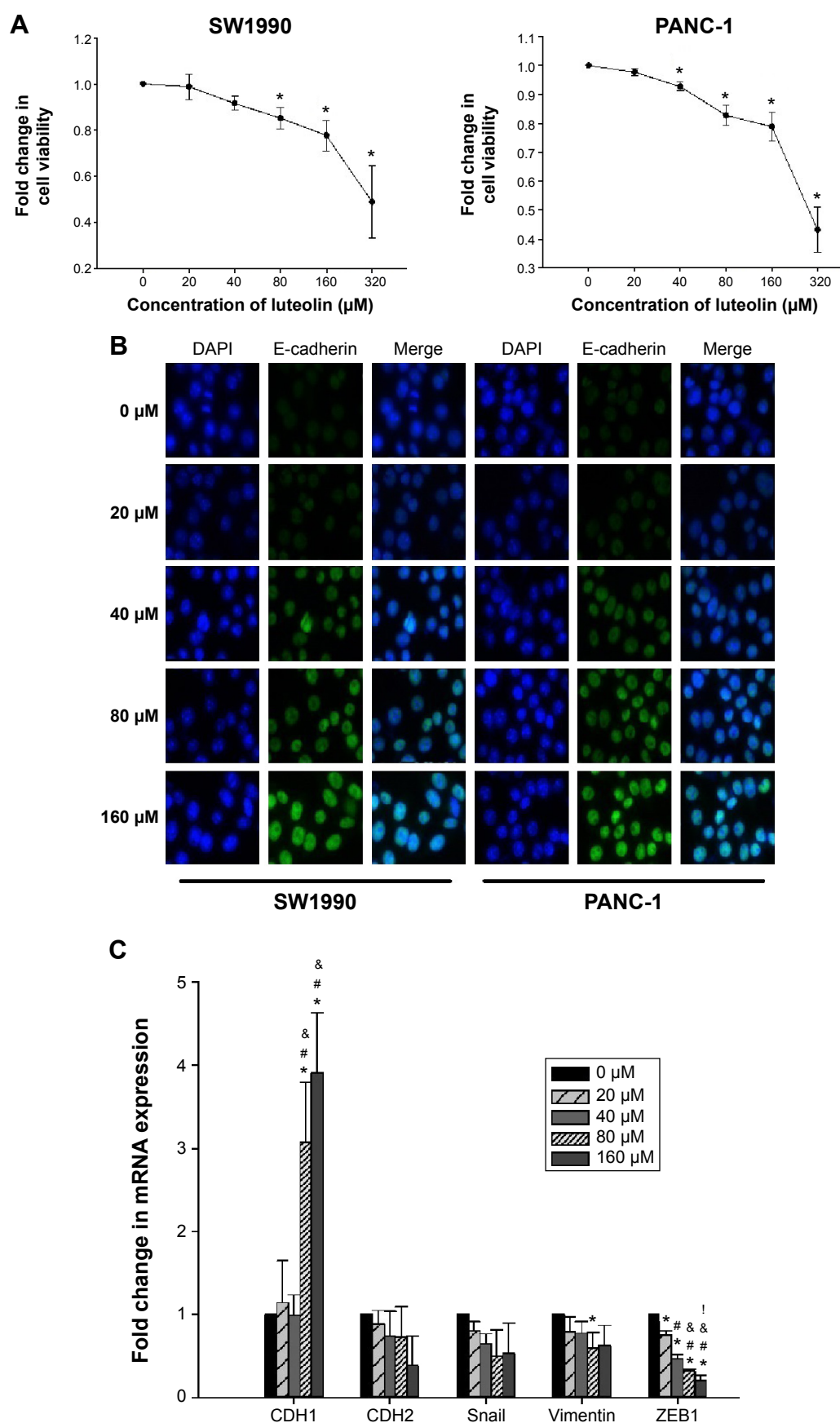
A

SW1990

PANC-1

B

SW1990

PANC-1
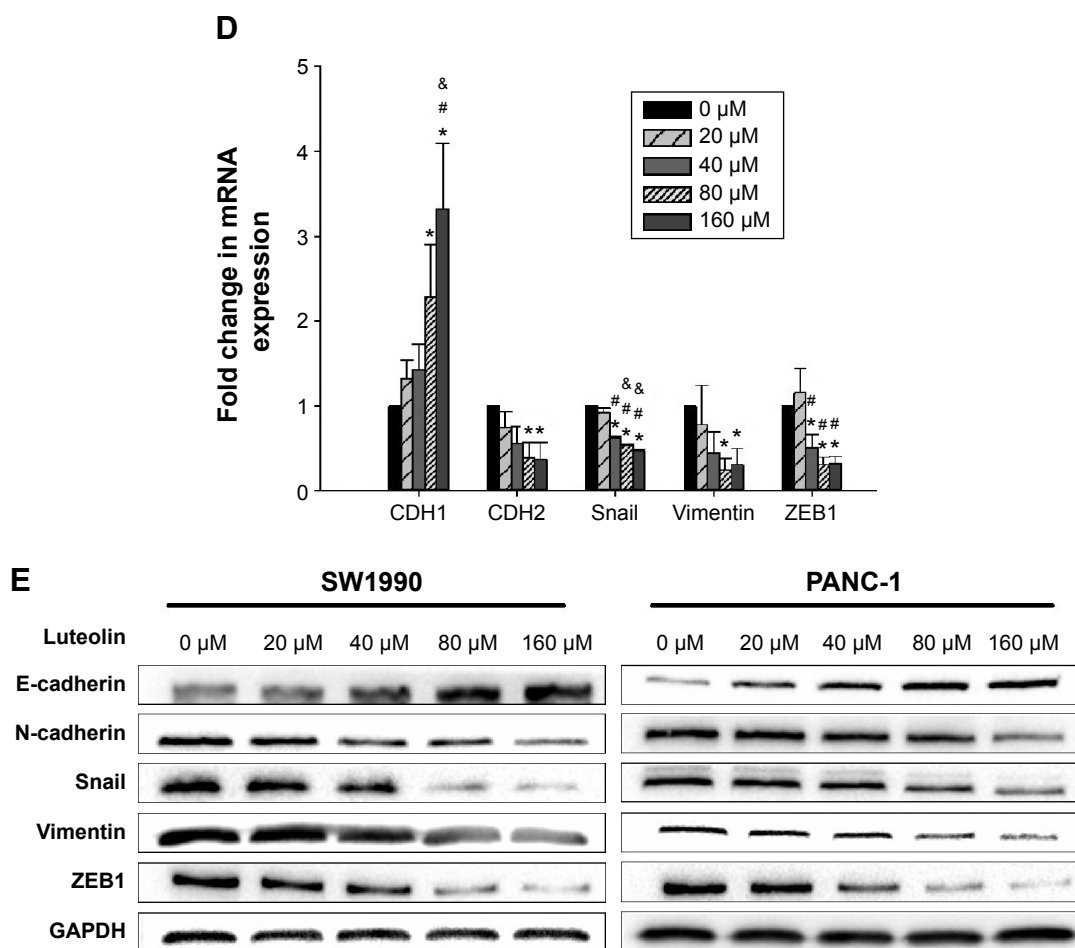
C

Figure 1 (*Continued*)

D

E

Figure 1 Luteolin decreases cell viability and inhibits EMT of PANC-1 and SW1990 cells in a dose-dependent manner.
Notes: Two cell lines were treated with luteolin at concentrations of 0, 20, 40, 80, and 160 μM for 24 hours. (**A**) Fold change in cell viability of SW1990 and PANC-1 cells. (**B**) Single and merged images show immunofluorescence staining of E-cadherin (green). The cell nucleus is stained blue by DAPI. (**C**) Fold change in mRNA expression of CDH1 (E-cadherin), CDH2 (N-cadherin), Snail, vimentin, and ZEB1 in SW1990 cells. (**D**) Fold change in mRNA expression of CDH1 (E-cadherin), CDH2 (N-cadherin), Snail, vimentin, and ZEB1 in PANC-1 cells. (**E**) Western blotting assay was performed to determine protein levels of E-cadherin, N-cadherin, Snail, vimentin, and ZEB1; GAPDH was used as an internal control. Data represent mean ± SEM, n=3, *$P<0.05$ vs 0 μM group; #$P<0.05$ vs 20 μM group; &$P<0.05$ vs 40 μM group; ᶦ$P<0.05$ vs 80 μM group.
Abbreviations: EMT, epithelial–mesenchymal transition; DAPI, 4′,6-diamidino-2-phenylindole; mRNA, messenger RNA; SEM, standard error of mean; GAPDH, glyceraldehyde 3-phosphate dehydrogenase.

pictures of three fields of each filter, and each field was equally divided into nine pictures. For every field, three pictures were randomly chosen and so for every filter nine pictures were used for cell counting. Average cell number per picture represents the invasiveness of cancer cells. In general, results of Transwell invasiveness assay accorded with MMP expression level, and luteolin showed inhibition against pancreatic cancer cell invasiveness (Figure 2D and E).

Luteolin deactivates p-STAT3 and inhibits the transcription of STAT3

Next, we determined the STAT3 activity of PANC-1 and SW1990 cells after luteolin treatment. By Western blotting assay, phosphorylated STAT3 (p-STAT3) level was determined after different concentrations of luteolin exposure. We observed luteolin powerfully deactivating p-STAT3 as p-STAT3 decreased much more dramatically than

EMT-related makers and MMPs with increase of luteolin concentration. And, when concentrations of luteolin reached 80 μM, p-STAT3 could almost not be detected on both cell types (Figure 3A).

During the process of STAT3 activity analysis, we also found that luteolin could downregulate the total amount of STAT3 in a dose-dependent manner. After verification by Western blotting assays, we performed PCR assays, and both results were in agreement (Figure 3A and B).

Luteolin reverses IL-6-induced EMT of PANC-1 and SW1990 cell lines

IL-6 has been confirmed as a cytokine that can induce EMT and promote pancreatic cancer cell invasion by activation of STAT3 signaling.[23,24] Since STAT3 activity was inhibited by luteolin in a dose-dependent manner, we sought to investigate whether luteolin could reverse IL-6-induced EMT of
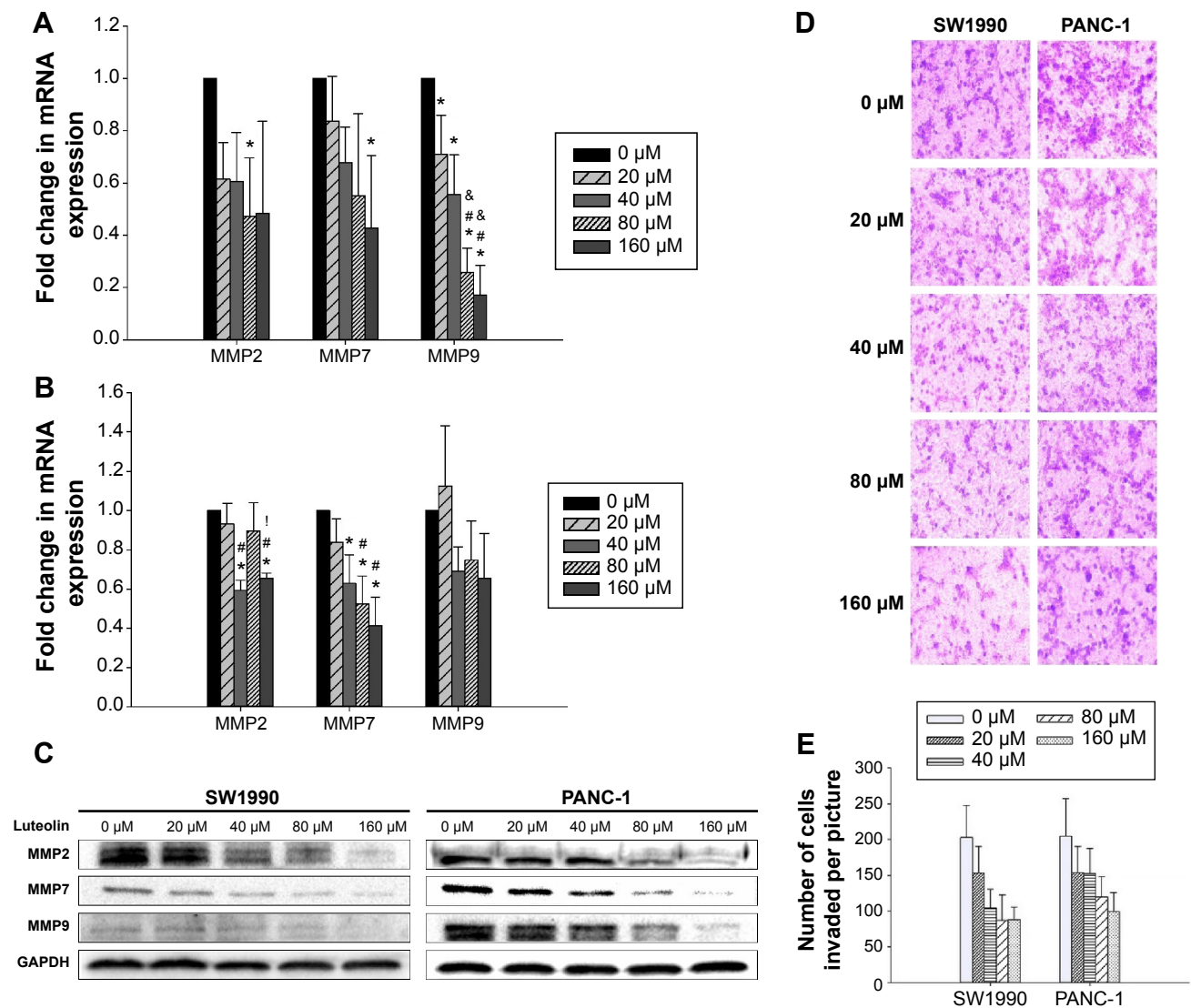
Figure 2 Luteolin inhibits MMP secretion and cell invasiveness of PANC-1 and SW1990 cells in a dose-dependent manner.
Notes: Two cell lines were treated with luteolin at concentrations of 0, 20, 40, 80, and 160 μM for 24 hours. (**A**) Fold change in mRNA expression of MMP2, MMP7, and MMP9 in SW1990 cells. (**B**) Fold change in mRNA expression of MMP2, MMP7, and MMP9 in PANC-1 cells. (**C**) Western blotting assay was performed to determine protein levels of MMP2, MMP7, and MMP9; GAPDH was used as an internal control. (**D** and **E**) Luteolin inhibited the invasive capacity of PANC-1 and SW1990 cells. The results are presented as the mean ± SD of experiments performed in triplicate. Data represent mean ± SEM, n=3, *$P<0.05$ vs 0 μM group; #$P<0.05$ vs 20 μM group; &$P<0.05$ vs 40 μM group; !$P<0.05$ vs 80 μM group.
Abbreviations: mRNA, messenger RNA; SEM, standard error of mean; MMPs, metalloproteinases; SD, standard deviation.

pancreatic cancer cells. PANC-1 and SW1990 cells were treated with IL-6 at a concentration of 100 ng/mL for 72 hours and in the last 24 hours, luteolin was added to the FBS-free medium to reach a concentration of 80 μM. We performed PCR assay to determine the change of CDH1 (E-cadherin), CDH2 (N-cadherin), Snail, vimentin, and ZEB1. CDH1 decreased after IL-6 treatment and the four mesenchymal biomarkers increased. Changes in these five EMT-related markers indicated mesenchymal transition of pancreatic cancer cells. But, this effect was inhibited by luteolin. When cells were cotreated with IL-6 and luteolin, IL-6-induced changes of EMT-related markers were effectively inhibited by luteolin (Figure 4A and B).

Then, we performed Western blotting assay, and the results were generally consistent with PCR assay (Figure 4C). We also observed that, morphologically, IL-6 caused a mesenchymal transformation in pancreatic cancer cells and that this transformation was reversed by luteolin (Figure 4D). All of these evidence confirmed that luteolin could reverse IL-6-induced EMT of pancreatic cancer cells.

Luteolin inhibits IL-6-induced MMP secretion of PANC-1 and SW1990 cell lines

Subsequently, we sought to uncover whether luteolin could inhibit IL-6-induced MMP secretion of PANC-1 and SW1990
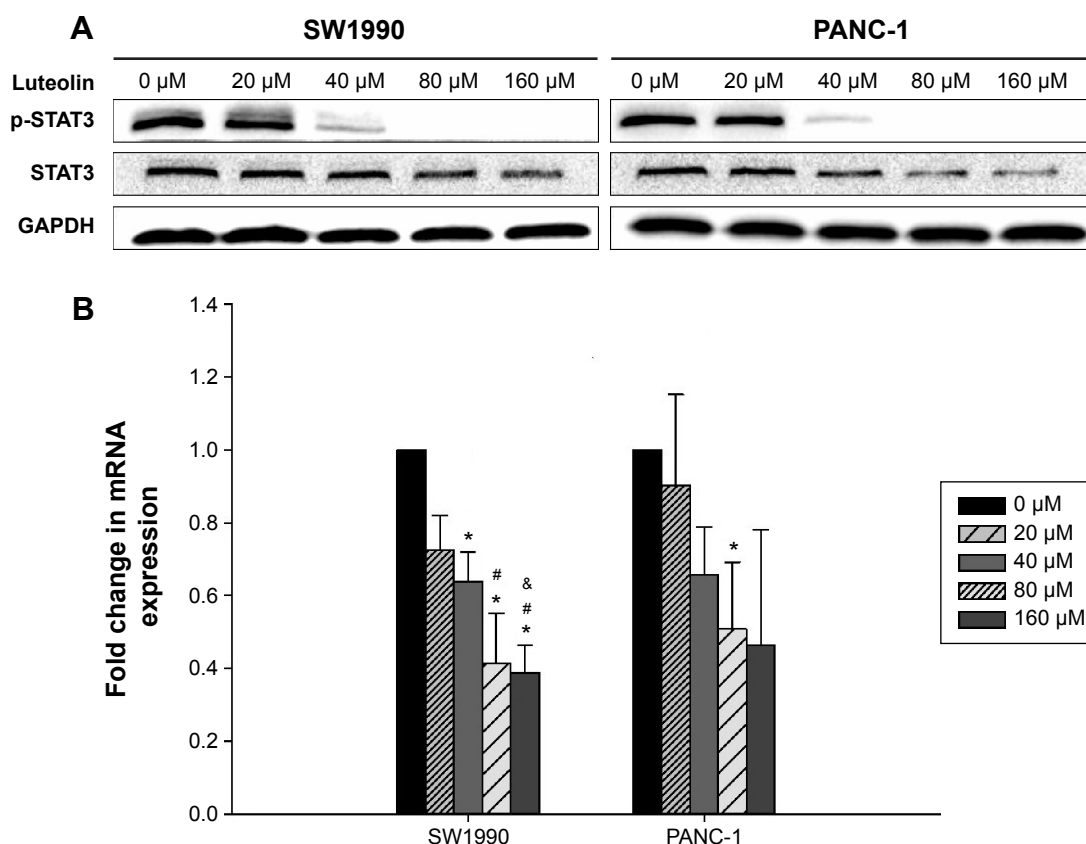
A

B

Figure 3 Luteolin deactivates p-STAT3 and inhibits the transcription of STAT3 of SW1990 and PANC-1 cell in a dose-dependent manner.
Notes: (**A**) Western blotting assay was performed to determine protein levels of p-STAT3 (Tyr705) and STAT3; GAPDH was used as an internal control. (**B**) Fold change in mRNA expression of STAT3 in SW1990 and PANC-1 cells. Data represent mean ± SEM, n=3, *$P<0.05$ vs 0 μM group; #$P<0.05$ vs 20 μM group; &$P<0.05$ vs 40 μM group; $^{l}P<0.05$ vs 80 μM group.
Abbreviations: mRNA, messenger RNA; SEM, standard error of mean; STAT3, signal transducer and activator of transcription 3; GAPDH, glyceraldehyde 3-phosphate dehydrogenase.

cells. Cells were treated as mentioned above. Western blotting and PCR assays were performed to determine MMP2, MMP7, and MMP9 levels. MMPs increased when treated with only IL-6 and decreased when treated with only luteolin. Moreover, luteolin effectively inhibited IL-6-induced increase of MMPs (Figure 5A–C). So, we concluded that luteolin inhibits IL-6-induced MMP secretion of PANC-1 and SW1990 cell lines.

When performing Western blotting assay, we also found that IL-6-induced STAT3 activation was effectively inhibited by luteolin. P-STAT3 showed the same variation trend as mesenchymal markers and MMPs (Figures 4C and 5A). As p-STAT3 is inhibited by luteolin effectively, we speculated that luteolin inhibits EMT and MMP secretion likely through deactivation of STAT3 signaling. But this speculation needs further study to be confirmed.

Discussion

Pancreatic cancer is perceived as one of the most invasive tumor diseases with disastrous prognoses. Surgery is considered the only method for radical treatment, but most patients have missed the opportunity for surgery by the time of diagnosis. Various biomarkers, indicating a poor prognosis have been found, such as *SMAD4* gene mutations, *K-ras* gene mutations, and upregulation of *CA19-9*.[32–34] However, little can be done with these indications. The prognosis has not been improved significantly despite emerging chemotherapy, radiotherapy, and biotherapy treatments. It has been reported that luteolin has the potential to be a new therapeutic agent for pancreatic cancer. Johnson et al[35] reported that combined treatment of luteolin and gemcitabine promoted apoptotic cell death in pancreatic tumor cells in vivo through inhibition of the K-ras/GSK-3β/NF-κB signaling pathway. Cai et al[36] reported that luteolin inhibits vascular endothelial growth factor secretion and angiogenesis of pancreatic cancer. Besides, luteolin has also been reported to promote apoptosis of pancreatic cancer cells by blocking epithelial growth factor receptor tyrosine kinase.[37] Here we found that luteolin decreased invasiveness of pancreatic cancer cell and further confirmed luteolin's potential to be a new therapeutic agent
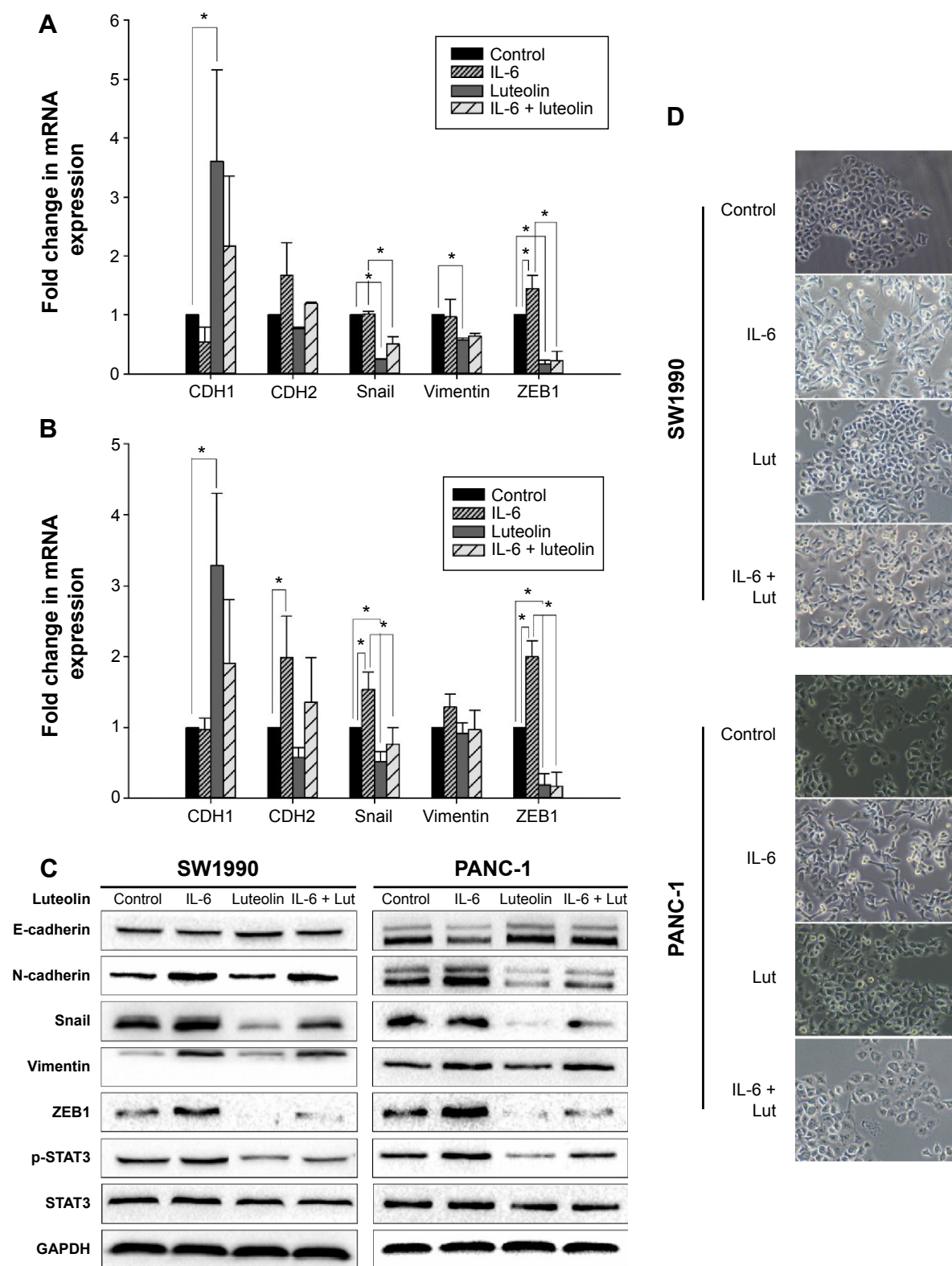
Figure 4 Luteolin reverses IL-6-induced EMT of PANC-1 and SW1990 cell lines.
Notes: Two cell lines were treated with IL-6 at 100 ng/mL for 72 hours in FBS-free media and in the last 24 hours luteolin was added to reach a concentration of 80 µM. (**A**) Fold change in mRNA expression of CDH1 (E-cadherin), CDH2 (N-cadherin), Snail, vimentin, and ZEB1 in SW1990 cells. (**B**) Fold change in mRNA expression of CDH1 (E-cadherin), CDH2 (N-cadherin), Snail, vimentin, and ZEB1 in PANC-1 cells. (**C**) Western blotting assay was performed to determine protein level of E-cadherin, N-cadherin, Snail, vimentin, and ZEB1; GAPDH was used as an internal control. (**D**) Morphological change of SW1990 and PANC-1 cells after treatment. Data represent mean ± SEM, n=3, *$P < 0.05$.
Abbreviations: mRNA, messenger RNA; SEM, standard error of mean; STAT3, signal transducer and activator of transcription 3; IL-6, interleukin-6; EMT, epithelial–mesenchymal transition; FBS, fetal bovine serum; GAPDH, glyceraldehyde 3-phosphate dehydrogenase.
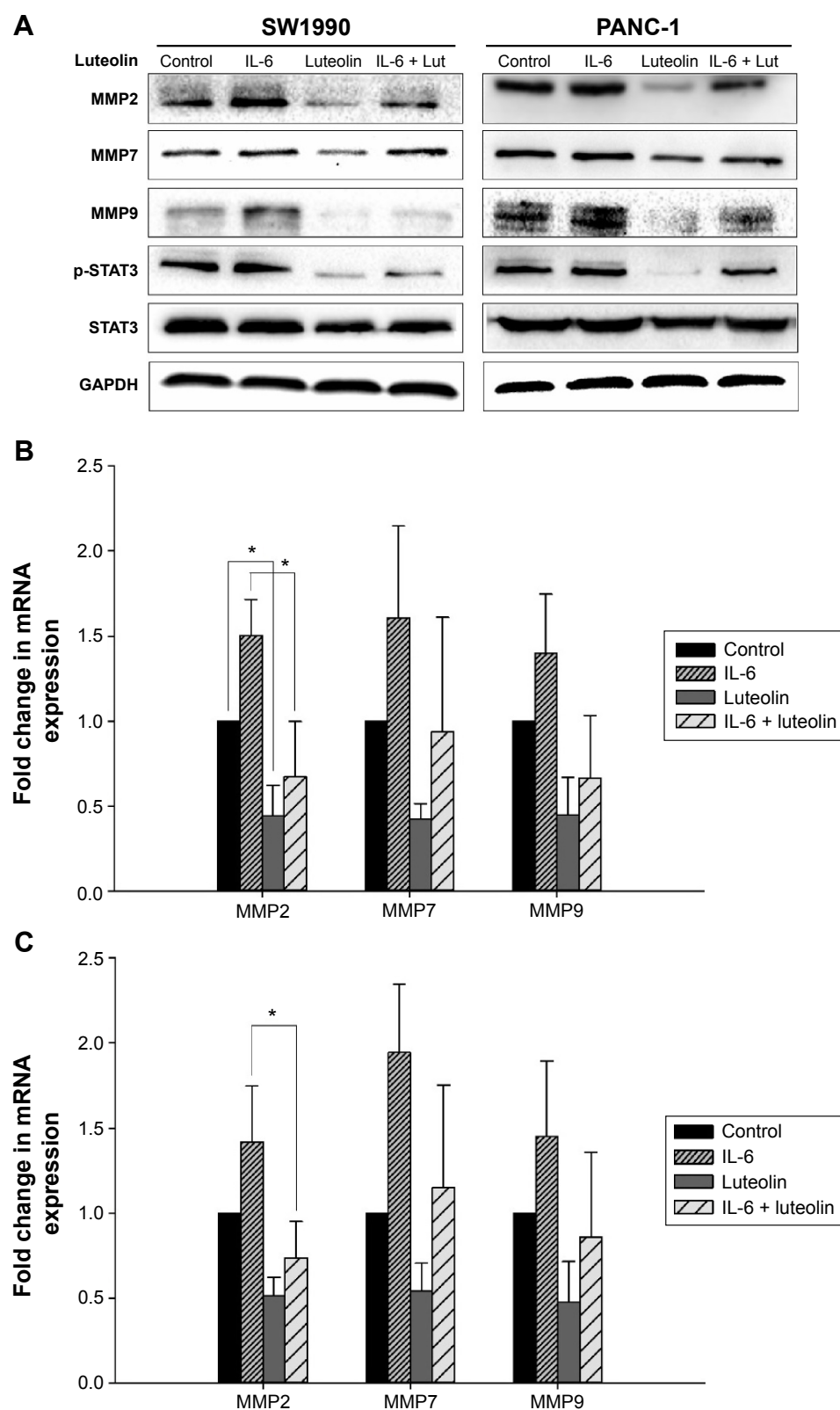
Figure 5 Luteolin inhibits IL-6-induced MMP secretion of PANC-1 and SW1990 cell lines.

Notes: Two cell lines were treated with IL-6 at 100 ng/mL for 72 hours in FBS-free media and in the last 24 hours luteolin was added to reach a concentration of 80 µM. (**A**) Western blotting assay was performed to determine protein level of MMP2, MMP7, and MMP9; GAPDH was used as an internal control. (**B**) Fold change in mRNA expression of MMP2, MMP7, and MMP9 in SW1990 cells. (**C**) Fold change in mRNA expression of MMP2, MMP7, and MMP9 in PANC-1 cells. Data represent mean ± SEM, n=3, *P<0.05.

Abbreviations: MMP, metalloproteinase; mRNA, messenger RNA; SEM, standard error of mean; STAT3, signal transducer and activator of transcription 3; IL-6, interleukin-6.

for pancreatic cancer. More than ten types of pancreatic cancer cell lines with various degrees of differentiation and invasiveness have been obtained from clinical patients, and some of them show EMT characteristics, which are downregulations of epithelial biomarkers and up-regulations of mesenchymal biomarkers. For instance, the PANC-1 cell line, which was used in our study, has been shown to have decreased expression of E-cadherin and a five-fold greater invasiveness than BxPC-3 cell line.[38,39] In our study, we found that both PANC-1 and SW1990 cell lines expressed high levels of Snail and vimentin, which are mesenchymal markers. Therefore, we hypothesized that luteolin, which has shown antineoplastic activity in previous studies,[9,11–13] could inhibit their expression and reverse EMT. The results agreed with our expectations that luteolin indeed inhibited EMT in pancreatic cancer cells. Previous studies have demonstrated that changes in EMT are often accompanied by increased expression of MMPs.[40,41] We therefore determined MMP2, MMP7, and MMP9 level after luteolin treatment and found that luteolin also effectively inhibited the expression of MMPs. By degrading extracellular matrix, MMPs make cancer cell migration possible.[42,43] So, we performed an in vitro Transwell invasiveness assay to established luteolin's inhibition on cancer cell invasiveness.

In our study, we observed that in PANC-1 and SW1990 cells, stimulation with IL-6 for 24 hours failed to cause significant EMT, either morphologically or in the results of Western blotting. As far as we know, IL-6 stimulation for 24 hours at a concentration of 100 ng/mL has been used successfully in a variety of cancer cells to induce EMT.[24,25] With an alteration from previous protocols, we finally succeeded in inducing EMT by stimulating with IL-6 for 72 hours in FBS-free medium. We inferred it was due to the high-level cell-autonomous phosphorylation of STAT3 in the two cell lines. As IL-6 works mainly through the JAK2/STAT3 pathway, high-level cell-autonomous phosphorylation of STAT3 may make exogenic IL-6 less decisive. STAT3 is becoming an increasingly important target for cancer treatment. As a powerful inhibitor of STAT3 signaling, luteolin has been uncovered to have the functions of antiproliferation, proapoptosis, and inhibition of metastasis.[8–12] Though it has not been proven to be a classic pathway interacting with EMT, STAT3 was shown to contribute to EMT through comprehensive alterations of transcription factors such as ZEB1.[44,45] Recently, Gujral et al[46] found that, in multiple Wnt5-Fzd2-expressing tumor cells, an unconventional mechanism of STAT3 activation drives EMT, cellular migration, and invasion. Some agents

show potential against EMT in cancer cells by deactivating STAT3.[47] In our study, we observed that dephosphorylation of STAT3 was accompanied by the upregulation of E-cadherin and downregulation of mesenchymal biomarkers and MMPs. It was suggested that luteolin inhibits EMT and invasiveness of pancreatic cancer cell, at least partly, by deactivation of STAT3 signaling.

Various in vivo and in vitro studies have revealed that IL-6 contributes crucially to pancreatic cancer initiation and progression through the activation of STAT3.[48] In a mouse model with the mutant *Kras* gene, STAT3 signaling activated by IL-6 promotes pancreatic cancer cell metastasis and mediates pancreatic ductal adenocarcinoma development.[20,48] We can therefore expect that, by targeting STAT3 activation, luteolin can not only inhibit pancreatic cancer cell invasiveness in vitro, but also stop Kras-induced pancreatic ductal adenocarcinoma formation. Besides, luteolin may have potential clinical applications in combination with conventional biotherapies. Type I interferons (IFNs) play a role in the immunotherapy of pancreatic cancer, but its clinical use is limited partly because of activation of JAK2/STAT3 pathway.[49] It has been reported that combined application of IFN and STAT3 antagonist effectively inhibits pancreatic cancer cell proliferation.[50] We may expect that the same effect could be achieved with the combined use of IFN and luteolin.

Conclusion

Our findings suggested that luteolin was an effective STAT3 signaling inhibitor with antineoplastic potential. Our results provide an important insight for understanding the mechanism of the anticancer effect of luteolin. Because of the importance of STAT3 in tumorigenesis, luteolin may play an important role in antitumor strategies in the future.

Disclosure

The authors report no conflicts of interest in this work.

References

1. Nijveldt RJ, van Nood E, van Hoorn DE, Boelens PG, van Norren K, van Leeuwen PA. Flavonoids: a review of probable mechanisms of action and potential applications. *Am J Clin Nutr*. 2001;74(4):418–425.
2. Ross JA, Kasum CM. Dietary flavonoids: bioavailability, metabolic effects, and safety. *Annu Rev Nutr*. 2002;22:19–34.
3. Middleton E Jr, Kandaswami C, Theoharides TC. The effects of plant flavonoids on mammalian cells: implications for inflammation, heart disease, and cancer. *Pharmacol Rev*. 2000;52(4):673–751.
4. Wang T, Zhang JC, Chen Y, Huang F, Yang MS, Xiao PG. Comparison of antioxidative and antitumor activities of six flavonoids from Epimedium koreanum. *Zhongguo Zhong Yao Za Zhi*. 2007;32(8):715–718.
5. Kandaswami C, Lee LT, Lee PP, et al. The antitumor activities of flavonoids. *In Vivo*. 2005;19(5):895–909.

6. Jia Z, Nallasamy P, Liu D, et al. Luteolin protects against vascular inflammation in mice and TNF-alpha-induced monocyte adhesion to endothelial cells via suppressing IκBα/NF-κB signaling pathway. *J Nutr Biochem*. 2015;26(3):293–302.

7. Theoharides TC, Conti P, Economu M. Brain inflammation, neuropsychiatric disorders, and immunoendocrine effects of luteolin. *J Clin Psychopharmacol*. 2014;34(2):187–189.

8. Yang MY, Wang CJ, Chen NF, Ho WH, Lu FJ, Tseng TH. Luteolin enhances paclitaxel-induced apoptosis in human breast cancer MDA-MB-231 cells by blocking STAT3. *Chem Biol Interact*. 2014;213:60–68.

9. Shi RX, Ong CN, Shen HM. Luteolin sensitizes tumor necrosis factor-alpha-induced apoptosis in human tumor cells. *Oncogene*. 2004;23(46):7712–7721.

10. Hong Z, Cao X, Li N, et al. Luteolin is effective in the non-small cell lung cancer model with L858R/T790M EGF receptor mutation and erlotinib resistance. *Br J Pharmacol*. 2014;171(11):2842–2853.

11. Cai X, Ye T, Liu C, et al. Luteolin induced G2 phase cell cycle arrest and apoptosis on non-small cell lung cancer cells. *Toxicol In Vitro*. 2011;25(7):1385–1391.

12. Choi EM, Lee YS. Luteolin suppresses IL-1beta-induced cytokines and MMPs production via p38 MAPK, JNK, NF-kappaB and AP-1 activation in human synovial sarcoma cell line, SW982. *Food Chem Toxicol*. 2010;48(10):2607–2611.

13. Bagli E, Stefaniotou M, Morbidelli L, et al. Luteolin inhibits vascular endothelial growth factor-induced angiogenesis; inhibition of endothelial cell survival and proliferation by targeting phosphatidylinositol 3′-kinase activity. *Cancer Res*. 2004;64(21):7936–7946.

14. Yu H, Shen Y, Hong J, Xia Q, Zhou F, Liu X. The contribution of TGF-beta in Epithelial-Mesenchymal Transition (EMT): down-regulation of E-cadherin via snail. *Neoplasma*. 2015;62(1):1–15.

15. Nakajima S, Doi R, Toyoda E, et al. N-cadherin expression and epithelial-mesenchymal transition in pancreatic carcinoma. *Clin Cancer Res*. 2004;10(12 Pt 1):4125–4133.

16. Shaul YD, Freinkman E, Comb WC, et al. Dihydropyrimidine accumulation is required for the epithelial-mesenchymal transition. *Cell*. 2014;158(5):1094–1109.

17. Andreolas C, Kalogeropoulou M, Voulgari A, Pintzas A. Fra-1 regulates vimentin during Ha-RAS-induced epithelial mesenchymal transition in human colon carcinoma cells. *Int J Cancer*. 2008;122(8):1745–1756.

18. Nieto MA, Cano A. The epithelial-mesenchymal transition under control: global programs to regulate epithelial plasticity. *Semin Cancer Biol*. 2012;22(5–6):361–368.

19. Qian LW, Mizumoto K, Urashima T, et al. Radiation-induced increase in invasive potential of human pancreatic cancer cells and its blockade by a matrix metalloproteinase inhibitor, CGS27023. *Clin Cancer Res*. 2002;8(4):1223–1227.

20. Fukuda A, Wang SC, Morris JP, et al. Stat3 and MMP7 contribute to pancreatic ductal adenocarcinoma initiation and progression. *Cancer Cell*. 2011;19(4):441–455.

21. Ito H, Duxbury M, Benoit E, et al. Prostaglandin E2 enhances pancreatic cancer invasiveness through an Ets-1-dependent induction of matrix metalloproteinase-2. *Cancer Res*. 2004;64(20):7439–7446.

22. Nagakawa Y, Aoki T, Kasuya K, Tsuchida A, Koyanagi Y. Histologic features of venous invasion, expression of vascular endothelial growth factor and matrix metalloproteinase-2 and matrix metalloproteinase-9, and the relation with liver metastasis in pancreatic cancer. *Pancreas*. 2002;24(2):169–178.

23. Dehai C, Bo P, Qiang T, et al. Enhanced invasion of lung adenocarcinoma cells after co-culture with THP-1-derived macrophages via the induction of EMT by IL-6. *Immunol Lett*. 2014;160(1):1–10.

24. Sullivan NJ, Sasser AK, Axel AE, et al. Interleukin-6 induces an epithelial-mesenchymal transition phenotype in human breast cancer cells. *Oncogene*. 2009;28(33):2940–2947.

25. Huang C, Yang G, Jiang T, Zhu G, Li H, Qiu Z. The effects and mechanisms of blockage of STAT3 signaling pathway on IL-6 inducing EMT in human pancreatic cancer cells in vitro. *Neoplasma*. 2011;58(5):396–405.

26. Chen Y, Deng J, Fujimoto J, et al. Gprc5a deletion enhances the transformed phenotype in normal and malignant lung epithelial cells by eliciting persistent Stat3 signaling induced by autocrine leukemia inhibitory factor. *Cancer Res*. 2010;70(21):8917–8926.

27. Cui W, Liu Y, Weinstein JS, Craft J, Kaech SM. An interleukin-21-interleukin-10-STAT3 pathway is critical for functional maturation of memory CD8+ T cells. *Immunity*. 2011;35(5):792–805.

28. Zhang Y, Du XL, Wang CJ, et al. Reciprocal activation between PLK1 and Stat3 contributes to survival and proliferation of esophageal cancer cells. *Gastroenterology*. 2012;142(3):521–530; e523.

29. He Z, He X, Chen Z, et al. Activation of the mTORC1 and STAT3 pathways promotes the malignant transformation of colitis in mice. *Oncol Rep*. 2014;32(5):1873–1880.

30. Baumgart S, Chen NM, Siveke JT, et al. Inflammation-induced NFATc1-STAT3 transcription complex promotes pancreatic cancer initiation by KrasG12D. *Cancer Discov*. 2014;4(6):688–701.

31. Corcoran RB, Contino G, Deshpande V, et al. STAT3 plays a critical role in KRAS-induced pancreatic tumorigenesis. *Cancer Res*. 2011;71(14):5020–5029.

32. Blackford A, Serrano OK, Wolfgang CL, et al. SMAD4 gene mutations are associated with poor prognosis in pancreatic cancer. *Clin Cancer Res*. 2009;15(14):4674–4679.

33. Chen H, Tu H, Meng ZQ, Chen Z, Wang P, Liu LM. K-ras mutational status predicts poor prognosis in unresectable pancreatic cancer. *Eur J Surg Oncol*. 2010;36(7):657–662.

34. Bernhard J, Dietrich D, Glimelius B, et al. Estimating prognosis and palliation based on tumour marker CA 19-9 and quality of life indicators in patients with advanced pancreatic cancer receiving chemotherapy. *Br J Cancer*. 2010;103(9):1318–1324.

35. Johnson JL, Dia VP, Wallig M, Gonzalez de Mejia E. Luteolin and gemcitabine protect against pancreatic cancer in an orthotopic mouse model. *Pancreas*. 2015;44(1):144–151.

36. Cai X, Lu W, Ye T, et al. The molecular mechanism of luteolin-induced apoptosis is potentially related to inhibition of angiogenesis in human pancreatic carcinoma cells. *Oncol Rep*. 2012;28(4):1353–1361.

37. Lee LT, Huang YT, Hwang JJ, et al. Blockade of the epidermal growth factor receptor tyrosine kinase activity by quercetin and luteolin leads to growth inhibition and apoptosis of pancreatic tumor cells. *Anticancer Res*. 2002;22(3):1615–1627.

38. Zhang D, Ma X, Wu B, Cui P, Liu H, Lu Z. Effect of MSX2 interference on epithelial-mesenchymal transitions of pancreatic cancer cell line PANC-1. *Nan Fang Yi Ke Da Xue Xue Bao*. 2015;35(2):179–184.

39. Stahle M, Veit C, Bachfischer U, et al. Mechanisms in LPA-induced tumor cell migration: critical role of phosphorylated ERK. *J Cell Sci*. 2003;116(Pt 18):3835–3846.

40. Asuthkar S, Nalla AK, Gondi CS, et al. Gadd45a sensitizes medulloblastoma cells to irradiation and suppresses MMP-9-mediated EMT. *Neuro Oncol*. 2011;13(10):1059–1073.

41. Radisky DC, Levy DD, Littlepage LE, et al. Rac1b and reactive oxygen species mediate MMP-3-induced EMT and genomic instability. *Nature*. 2005;436(7047):123–127.

42. Lu W, Xia YH, Qu JJ, et al. p21-activated kinase 4 regulation of endometrial cancer cell migration and invasion involves the ERK1/2 pathway mediated MMP-2 secretion. *Neoplasma*. 2013;60(5):493–503.

43. Xu C, Hu DM, Zhu Q. eEF1A2 promotes cell migration, invasion and metastasis in pancreatic cancer by upregulating MMP-9 expression through Akt activation. *Clin Exp Metastasis*. 2013;30(7):933–944.

44. Balanis N, Wendt MK, Schiemann BJ, Wang Z, Schiemann WP, Carlin CR. Epithelial to mesenchymal transition promotes breast cancer progression via a fibronectin-dependent STAT3 signaling pathway. *J Biol Chem*. 2013;288(25):17954–17967.

45. Guo L, Chen C, Shi M, et al. Stat3-coordinated Lin-28-let-7-HMGA2 and miR-200-ZEB1 circuits initiate and maintain oncostatin M-driven epithelial-mesenchymal transition. *Oncogene*. 2013;32(45): 5272–5282.

46. Gujral TS, Chan M, Peshkin L, Sorger PK, Kirschner MW, MacBeath G. A noncanonical Frizzled2 pathway regulates epithelial-mesenchymal transition and metastasis. *Cell*. 2014;159(4):844–856.

47. Lu Z, Wang J, Zheng T, et al. FTY720 inhibits proliferation and epithelial-mesenchymal transition in cholangiocarcinoma by deactivating STAT3 signaling. *BMC Cancer*. 2014;14:783.

48. Lesina M, Kurkowski MU, Ludes K, et al. Stat3/Socs3 activation by IL-6 transsignaling promotes progression of pancreatic intraepithelial neoplasia and development of pancreatic cancer. *Cancer Cell*. 2011; 19(4):456–469.

49. Dicitore A, Caraglia M, Gaudenzi G, et al. Type I interferon-mediated pathway interacts with peroxisome proliferator activated receptor-γ (PPAR-γ): at the cross-road of pancreatic cancer cell proliferation. *Biochim Biophys Acta*. 2014;1845(1):42–52.

50. Vitale G, Zappavigna S, Marra M, et al. The PPAR-γ agonist troglitazone antagonizes survival pathways induced by STAT-3 in recombinant interferon-β treated pancreatic cancer cells. *Biotechnol Adv*. 2012; 30(1):169–184.